Novel Nanoparticle Contrast Agents for Magnetic Resonance Imaging

Edward Van Keuren[*], Sarah Stoll[**], Vidumin Dahanayake[**], Trevor Lyons[**], Priscilla Glaser[**], Olga Rodriguez[***], and Stanley Fricke[****], Christopher Albanese[****]

[*]Department of Physics, Georgetown University, Washington, DC, erv@georgetown.edu
[**]Department of Chemistry, Georgetown University
[***] Department of Oncology, Lombardi Comprehensive Cancer Center, Georgetown University Medical Center, Washington, D.C. 20057
[****] Department of Radiology, Georgetown University Medical Center, Washington, D.C. 20057

ABSTRACT

Magnetic resonance imaging (MRI) is an important diagnostic tool in both clinical and research environments. In order to improve imaging sensitivity, contrast agents (CAs) are often administered prior to or during imaging sessions. We have been developing a number of novel nanoparticle-based CAs consisting of metal-oxo clusters with high spins (molecular magnets) encapsulated in polymer nanocarriers. The pure clusters show excellent relaxivities, which can be further enhanced by encapsulation in the polymers. In some cases, values comparable to or larger than those of commercially available CAs can be achieved.

Keywords: magnetic resonance imaging contrast agents

1 BACKGROUND

Magnetic resonance imaging has become a fundamental diagnostic tool for clinicians and researchers [1]. Signal contrast weighting in MRI, among other physical parameters, depends on the MRI pulse-sequence-timing and relaxation rates of the magnetization of hydrogen atoms' protons, where the relaxation times T_1, T_2, or T_2*, depend on the type of tissue being imaged

In order to improve sensitivity and resolution, contrast agents (CAs) can be administered prior to or during imaging to act as dynamic contrast enhancing (DCE) agents. These materials will distribute inhomogeneously in the body, and affect the local spin relaxation rates of the water protons, leading to higher contrast [2, 3]. Numerous clinically approved CAs are available, in particular Gadolinium (Gd) chelates for T_1-weighted imaging and iron oxide nanoparticles for T_2-weighted imaging. The enhancement in imaging sensitivity enabled by CAs has spurred research into further improving their properties, as well as in investigating alternative materials. There are also concerns about adverse side effects for some of the commonly used agents, in particular, related to the leaching of the highly cyto-toxic rare-earth metals such as Gd that are used in many T_1 CAs [4]. These compounds have been associated with serious side effects, such as nephrogenic systemic fibrosis, a condition characterized by a thickening of connective tissue of the kidney that can be fatal [5].

For over a decade, we in the Center for Translational Imaging (CTI) have been developing alternative MRI contrast agents based on metal-oxo clusters containing manganese and/or iron [6-10]. The high spin states of these "single molecule magnets" (SMMs) has led to them being extensively studied for applications in data storage and spintronics [11], but we have shown that they can also provide large contrast enhancement in MRI. In order to stabilize them for physiologically relevant environments, as well as to provide a convenient platform for targeting specific tissue, we used miniemulsion polymerization to encapsulate the clusters into polymer nanoparticles. Miniemulsion polymerization is a facile method for embedding various chemical species into polymer nanoparticles during the polymerization process [12]. This method produces particles with diameters on the order of 50~200 nm with narrow size distributions. We have successfully encapsulated several different types of metal-oxo clusters into polymers, including polystyrene and polyacrylamide, and shown that they provide excellent contrast enhancement in both T_1 and T_2 weighted MR images.

2 MATERIAL SYNTHESIS

2.1 Sample preparation

Various metal-oxo clusters were prepared according to procedures outlined in the literature [7, 13, 14]. In some cases, a ligand exchange was done in order to incorporate the cluster into the polymer backbone. The structures of some of the clusters we investigated are shown in Figure 1.

The polymer nanoparticles were made using the method of miniemulsion polymerization, as depicted in Figure 2. Clusters were mixed with monomers, e.g. styrene, cross-linkers such as divinyl benzene, a polymerization initiator, and a strong hydrophobe such as hexadecane, which prevents Ostwald ripening of the emulsion droplets. This solution was then combined with an aqueous solution

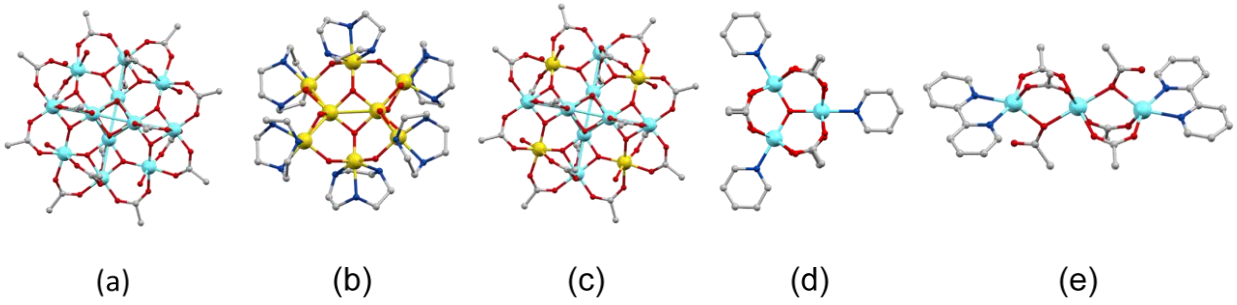

Figure 1: Metal-oxo clusters: (a) $Mn_{12}O_{12}(O_2CCH_3)_{16}(H_2O)_4$ (=Mn_{12}), (b) $Fe_8(tacn)_6O_2$-$(OH)_{12}Br_8$ (=Fe_8, tacn=1,4,7-triazacyclononane,), (c) $Mn_8Fe_4O_{12}(O_2CCH_3)_{16}(H_2O)_4$ (=Mn_8Fe_4), (d) $Mn_3O(O_2CCH_3)_6(pyr)_2$ (=Mn_3-pyr, pyr = pyridyl) (e) $Mn_3(O_2CCH_3)_6(Bpy)_2$ (Mn_3bpy, Bpy = bipyridyl).

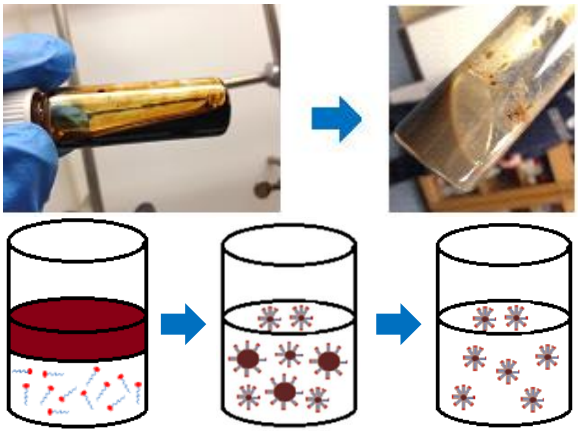

Figure 2: Mn_8Fe_4 clusters in solution (top left) and encapsulated in polystyrene nanoparticles (top right. Schematic diagram of miniemulsion polymerization: phase separated monomer and water containing surfactant (bottom left), pre-emulsified suspension (bottom middle), polymerized particles suspended in water (bottom right).

containing a surfactant such as SDS, then emulsified using a high-powered ultrasonic transducer. The emulsion is metastable, but before it can phase separate, polymerization is initiated by raising the temperature to 60°C under gentle agitation for 6 hours. The resulting nanoparticle dispersions were purified using dialysis.

2.2 Characterization

Particle sizes were measured using a dynamic light scattering apparatus based on an ALV-5000 (ALV GmbH, Germany) autocorrelator and custom-built optics. Relaxation data was collected in a 9.4 T Varian MR 400 MHz spectrometer using standard 5 mm quartz tubes. Phantom and in-vivo imaging was performed on a 7T Bruker Biospin (Germany/USA), using sequences and timing as described in references 6-10.

3 RESULTS AND DISCUSSION

The clusters alone showed good relaxivity values (relaxivity is defined as the inverse relaxation time normalized to the concentration of metal atoms in the clusters). The prototypical SMM, Mn_{12}, displayed a considerable relaxivity, considering that it contained no divalent manganese. Even larger values were found for other clusters, in particular for the transverse relaxivity r_2, as shown in Table 1. The values for Gd DTPA, (Magnevist, Bayer HealCare AG) a commonly used CA, are also shown for reference.

We were able to successfully incorporate the Mn_{12} [6, 7] and Mn_8Fe_4 [8] clusters into polystyrene nanoparticles using miniemulsion polymerization, shown previously in Figure 2. In this case, ligand substitution on the cluster to vinylbenzoic acid enabled the cluster to be chemically linked into the polymer chain. We obtained particle sizes on the order of 70~80 nm in diameter with narrow size distributions. These materials showed good contrast enhancement in T_1-weighted images, acquired on the 7T Bruker MRI in the Georgetown-Lombardi Preclinical Imaging Research Laboratory, as shown in Figure 3 for Mn_8Fe_4-co-polystyrene.

Cluster/system	**Relaxivity (mM-1 metal s-1)**	
	r_1	r_2
Mn_{12}	0.43	2.9
Mn_8Fe_4	2.3	29.5
Fe_8	4.76	5.01
Mn_3-pyr	19.0	155.8
Mn_3-bpy	12.4	145.0
Gd DTPA (Magnevist)	4.5	5.96

Table 1: Cluster relaxivities measured at 9.4 T.

Due to the good solubility in water of the Mn_3-bpy cluster, it was encapsulated into polyacrylamide using an inverse miniemulsion polymerization [9]. Somewhat larger

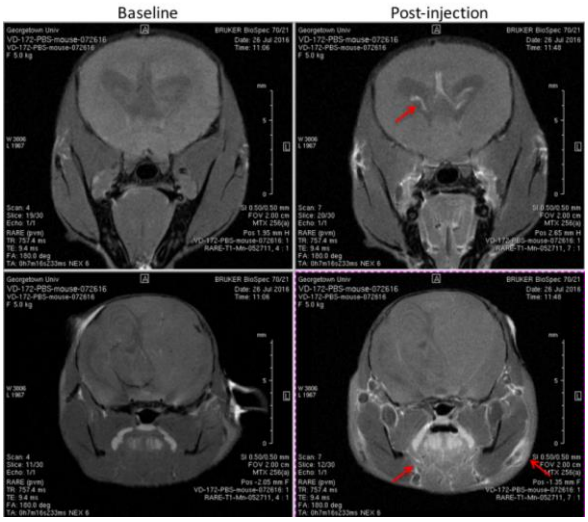

Figure 3: Baseline and post-injection scans of mouse brains The top and bottom images are different image slices. The red arrows indicate increased contrast in the choroid plexus of the inter-ventricular region (top) and muscle (bottom).

particles were obtained (~125 nm diameter) which further swelled when suspended in an aqueous environment.

In all cases the relaxivities were significantly affected by encapsulation into nanoparticles. For Mn_8Fe_4, r_1 increased from 2.4 mM^{-1} metal s^{-1} in the pure cluster to 3.4 mM^{-1} metal s^{-1} in the nanoparticle, while r_2 decreased from 27.7 to 11.2 mM^{-1} metal s^{-1}. Mn_3-bpy, on the other hand, showed a more significant increases in r_1 when encapsulated in polyacrylamide, going from 12.4 to 54.4 mM^{-1} metal s^{-1}, while r_2 remained essentially constant at around 145 mM^{-1} metal s^{-1}. This value for r_1 is more than an order of magnitude larger than that of commercial T_1 contrast agents, while the r_2 value is similar to that of commercial T_2 agents, making this material extremely interesting as a dual-mode contrast agent.

We have also done extensive work investigating the stability, biodistribution, and pharmacokinetics of the cluster/nanocarriers [9, 10]. Solution stability and metal leaching of the polystyrene and polyacrylamide nanocomposites were evaluated in various biological solutions. Both nanocomposites exhibit metal leaching of less than 0.35%, concentrations, well below the lowest toxicity reported in blood. *In vivo* particle integrity of Mn_8Fe_4coPS-IO was assessed via x-ray fluorescence spectroscopy. High correlations of iron and manganese in comparison to the endogenous control are indicative of beads maintaining their integrity *in vivo*.

4 CONCLUSIONS

We have shown that our cluster/nanocarriers have great potential for use as MRI contrast agents while potentially minimizing possible impacts of Gd-based CAs on tissues such as the kidney. The relatively simple and scalable synthesis, the wide variety of possible clusters and polymer nanocarriers, and the ability to modify the polymer surfaces make this a promising platform for future advances in the development of highly sensitive, low toxicity MRI contrast agents.

REFERENCES

[1] Bushong, S. C.; Clarke, G. D. *Magnetic resonance imaging:physical and biological principles;* Elsevier Mosby: St. Louis, Missouri, 2015.

[2] Wahsner, J.; Gale, E. M.; Rodríguez-Rodríguez, A.; Caravan, P. "Chemistry of MRI Contrast Agents: Current Challenges and New Frontiers" *Chem. Rev.* **2019**, *119*, 957-1057.

[3] Caspani, S.; Magalhães, R.; Araújo, J. P.; Sousa, C. T. "Magnetic Nanomaterials as Contrast Agents for MRI" *Materials* **2020**, *13*, 2586.

[4] Rogosnitzky, M.; Branch, S.; Rogosnitzky, M. "Gadolinium-Based Contrast Agent Toxicity: A Review of Known and Proposed Mechanisms" *Biometals* **2016**, *29*, 365-376.

[5] Broome, D. R. "Nephrogenic Systemic Fibrosis Associated with Gadolinium Based Contrast Agents: A Summary of the Medical Literature Reporting" *Eur. J. Radiol.* **2008**, *66*, 230-234.

[6] Mertzman, J. E.; Kar, S.; Lofland, S.; Fleming, T.; Van Keuren, E.; Tong, Y. Y.; Stoll, S. L. "Surface Attached Manganese-Oxo Clusters as Potential Contrast Agents" *Chemical communications (Cambridge, England)* **2009**, 788-790.

[7] Pablico, M. H.; Mertzman, J. E.; Japp, E. A.; Boncher, W. L.; Nishida, M.; Van Keuren, E.; Lofland, S. E.; Dollahon, N.; Rubinson, J. F.; Holman, K. T.; Stoll, S. L. "Miniemulsion Synthesis of Metal-Oxo Cluster Containing Copolymer Nanobeads" *Langmuir* **2011**, *27*, 12575-12584.

[8] Pablico-Lansigan, M.; Hickling, W. J.; Japp, E. A.; Rodriguez, O. C.; Ghosh, A.; Albanese, C.; Nishida, M.; Van Keuren, E.; Fricke, S.; Dollahon, N.; Stoll, S. L. "Magnetic Nanobeads as Potential Contrast Agents for Magnetic Resonance Imaging" *ACS Nano* **2013**, *7*, 9040-9048.

[9] Dahanayake, V.; Pornrungroj, C.; Pablico-Lansigan, M.; Hickling, W. J.; Lyons, T.; Lah, D.; Lee, Y.; Parasido, E.; Bertke, J. A.; Albanese, C.; Rodriguez, O.; Van Keuren, E.; Stoll, S. L. "Paramagnetic Clusters of $Mn_3(O_2CCH_3)_6(Bpy)_2$ in Polyacrylamide Nanobeads as a New Design Approach to a T_1-T_2 Multimodal Magnetic Resonance Imaging Contrast Agent" *ACS Appl. Mater. Interfaces* **2019**, *11*, 18153-18164.

[10] Dahanayake, V.; Lyons, T.; Kerwin, B.; Rodriguez, O.; Albanese, C.; Parasido, E.; Lee, Y.; Van Keuren, E.; Li, L.; Maxey, E.; Paunesku, T.; Woloschak, G.; Stoll, S. L. "Paramagnetic Mn_8Fe_4-Co-Polystyrene Nanobeads as a Potential T_1-T_2 Multimodal

Magnetic Resonance Imaging Contrast Agent with *In Vivo* Studies" *ACS Appl. Mater. Interfaces* **2021**, *13*, 39042-39054.

[11] Hołyńska, M., Ed., *Single-molecule magnets: molecular architectures and building blocks for spintronics;* Wiley-VCH: Weinheim, Germany, 2019.

[12] Landfester, K.; Bechthold, N.; Tiarks, F.; Antonietti, M. "Formulation and Stability Mechanisms of Polymerizable Miniemulsions" *Macromol.* **1999**, 5222-5228.

[13] Schake, A. R.; Tsai, H. L.; Webb, R. J.; Folting, K.; Christou, G.; Hendrickson, D. N. "High-Spin Molecules: Iron(III) Incorporation into $[Mn_{12}O_{12}(O_2CMe)_{16}(H_2O)_4]$ To Yield $[Mn_8Fe_4O_{12}(O_2CMe)_{16}(H_2O)_4]$ and Its Influence on the S = 10 Ground State of the Former" *Inorg. Chem.* **1994**, *33*, 6020–6028.

[14] Ménage, S.; Bergerat, P.; Codjovi, E.; Kahn, O.; Girerd, J. J.; Vitols, S. E.; Guillot, M.; Solans, X.; Calvet, T. "Structure of the linear trinuclear complex hexakis(acetato)bis(2,2'-bipyridine)trimanganese (II). Determination of the J electron-exchange parameter through magnetic susceptibility and high-field magnetization measurements" *Inorg. Chem.* **1991**, *30*, 2666–2671.